Vol. 10(36), Apr. 2020, PP. 4608-4624

Contents list available at IJMEC

International Journal of Mechatronics, Electrical and Computer Technology (IJMEC)

Journal Homepage: www.aeuso.org

PISSN: 2411-6173 - EISSN: 2305-0543

Development of an Experimental Robotic Test Bed for Unmanned Aerial Vehicle Control

EseOghene OVIE[1], Abdulkareem Bebeji IBRAHIM[2], Chichebe AKACHUKWU[1] and Olufemi AGBOOLA[2]

[1] AUAVL/NASRDA, [2] ESS/NASRDA

***Corresponding Author's E-mail:** oveseovese@gmail.com*

Abstract

This paper focuses on the control policy/law development for a nonlinear model of a quadrotor unmanned aerial vehicle (UAV). It identifies and implements three different control laws on the quadrotor UAV model viz-a-vis PID, Lyapunov and nonlinear backstepping controllers. Satisfactory results were obtained in attitude tracking simulation experiments for the three controllers. A first take at what constitutes good system response was made when response characteristics like rise time, settling time and peak overshoot were used. The Lyapunov controller outperformed both the standard PID in terms of no overshoot and also the nonlinear backstepping controller in terms of overshoot but performs poorly when rise time and steady state response time is considered. However considering energy conservation with torque as the operative variable, the nonlinear backstepping controller outperformed both the PID and Lyapunov controllers. This has made nonlinear controller selection and development the adopted control scheme for the long term goals of this project.

Keywords: Robotic systems, UAV, stabilization, tracking, full set of off the shelve UAV system with inbuilt multisensory camera, nonlinear control

1. Introduction

The demands for modern robotic systems are driven by their ability to simplify work and enable task execution at reduced cost [9]. Examples of such system span a wide range of classification and application areas, including factory or industrial, service, medical, hazardous environment, aerospace and construction robots [7], where the role of human operator or end user has been simplified and reduced with respect to involvement with task execution. In today's highly dynamic and fast paced socio-economic clime, robotic systems are fast replacing humans in certain types of activities. Such robots must however be developed within the scope of varying national and international interests, as the case may be [8] [10]. Consequently, different academic, industrial, military, political and ethical challenges exist with specific frameworks that makes them suitable for use and interaction in certain countries and not in others. However one unifying factor that drives robotic system development, is the need for continuous system compatibility with humans and other environmental factors within the robots' area of operation [13][7]. Some benefits of robotic application for solving problems include savings and conservation of material, personnel, energy, time and overall cost [8]. One of the ways to meet these sometimes stringent requirements is the development of highly efficient controllers for such robotic platforms.

2. Controller Classification

Article History:
Received Date: Mar. 03, 2019
Accepted Date: Aug. 16, 2019
Available Online: Apr. 01, 2020

Central to any robotic system's task description is the ability of the robot to adhere to well defined algorithms, which determine its behavior. These algorithms are otherwise known as control policies or laws. Realizations of which can be seen as software, usually programmable into any of the compatible microprocessor types and thereafter referred to as the controller [4]. Historically, controller development and their applications has evolved from classical to modern and more recently artificially intelligent and computationally intelligent heuristic algorithms [4].

2.1. Classical Controllers

Pre 1960, classical controllers which include the PID were the mainstay in numerous control applications. However, the decades following 1960 saw demand from aerospace industries for better performing controllers[4][6]. Especially as control system treatment progressed from simple linear single-input single-output (SISO) systems to multiple-input multiple-outpit(MIMO) system development and nonlinear considerations.

2.2. Modern Controllers

This renewed demand for robust, adaptive and optimal controllers gave rise to modern controllers such as LQR, LQG, H2, Hinf, sliding mode, state and output feedback controllers [7], immersion invariance[3]. These modern controllers have become a mainstay of any nonlinear system requiring automatic control [11] [23]. The nonlinear controllers are better suited to take care of the inherent nonlinearities found in most systems to be controlled [9] [5] compared to their linear classical variants. Although nonlinear controllers are more complex than their linear counterparts, they are better representatives of the true nature of most dynamic models being studied [9]. Most dynamic systems and models obey inherently nonlinear physical laws and are better described using nonlinear physical models. Applying nonlinear controllers to these systems offers; good robustness, adaptability and more degrees of design freedom to fine-tune and refine the system parameters either offline or in real-time via optimal control laws [24].

2.3. Optimum Control using Nature Inspired Algorithms

Controller evolution has received new impetus with adoption of artificial intelligence (AI) and computational intelligence (CI) techniques. These techniques which employ nature inspired algorithms, has opened up new and interesting developments in controller design [8]. Some of these AI tools applied to robotic systems include neural networks, particle swarm optimization, genetic algorithm, fuzzy logic, ant colony optimization, bee colony optimization, fire fly, bat algorithm, smell agent, Artificial fish swarm [2] etc. These techniques are understood [20] [14] to form optimization tools. Although not given to full mathematical deductive and inductive analyses, utilize heuristic rules that give satisfactory results [12]. They have proven efficient at counteracting the deficiencies of traditional linear and nonlinear controllers, especially where parametric and nonparametric uncertainties are factors considered in the system under control [23]. Uncertainties being causative factor in performance degradation that is visible and quantifiable in unacceptable error margins seen in system response to inputs and deviation from set trajectory. More detailed review of different controller types and effect of feedback is well documented in [11] [23].

3. Research Aim, Objectives and Characterization

For this work, controllers used were developed for a nonlinear model of the quad-rotor therefore necessitating development of nonlinear controllers for the unmanned aerial vehicle (UAV) system. The concept is stabilization and regulation of selected system states while identifying the control torque behavioral response of each selected controller type. To this end, three control laws are described viz-a-vis PID, Lyapunov and nonlinear backstepping controllers.

The UAV project aims for the development of energy efficient unmanned platforms that can operate in highly dynamic environments. At its core, the UAV can reliably generate data and serve as a platform for knowhow technology transfer for academic researchers and industry practitioners in robotics development of UAV's.

The current research interest for UAV design is driven by a national policy for sustainable development of robotic systems that are unmanned and self-supervised. In order to effectively demonstrate the UAV model in this paper, a multisensory lightweight Gyro-stabilized drone camera concept has been adopted. The camera payload will be deployed on board the UAV system, which can provide aerial photography or video recordings.

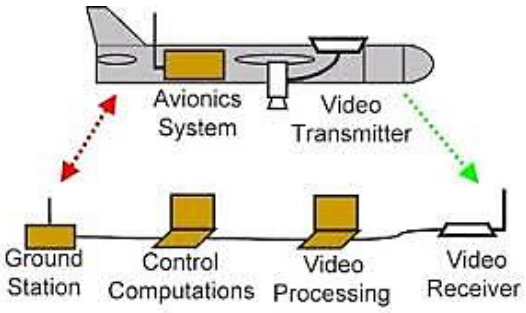

Figure 1: Proposed Operational Framework for Complete UAVS

Figure 1 depicts this concept with the various system parts and their relationship with each other shown. Figure 1 shows the UAV, two-way communication system, payload processing equipment of ground station, guidance, navigation and control (GNC) system. The choice for such a UAV however has been motivated by prevailing events in the country. Some areas of application of the work in this paper are but not limited to uses which meet certain critical national needs like security, surveillance, agriculture, disaster management, geographical mapping, and safety inspection. Other targeted users include film makers and journalist, service delivery and logistics companies. Ultimately, an indigenous technological capacity for robotic systems development will be engendered such that other industries spring up from it as spinoffs for other consumer products.

The authors are optimistic that with the convincing results obtained during computer simulations as demonstrated in this paper, there is no doubt that advanced stages of this work considering full implementation will be greatly enhanced by the knowledge gained. The final flight model will also benefit from rigorous control law testing, verification and hardware validation with appreciable performance margins in energy savings and overall system behavior expected from utilized controllers.

The arrangement of the rest of the paper is as follows: conceptual design is presented in Section II, Section III presents the QUAV model while Section IV addresses controller synthesis. Section V presents the results and goes on to analyze obtained results while section VI concludes the paper.

4. Conceptual Design of System

Similar to work done in [17], this project has as objective development of UAV systems for academic and research purposes. Furthermore, the project aims to bring UAV systems that are developed and engineered with purely homegrown competency to the use of the general public with particular focus areas being security, surveillance, agriculture, disaster management and other industrial uses.

4.1. Program workflow

One particular workflow for achieving the proposed concept and mandate has been given in Figure 2. This roadmap forms a working template for relevant actors in the UAVS project.

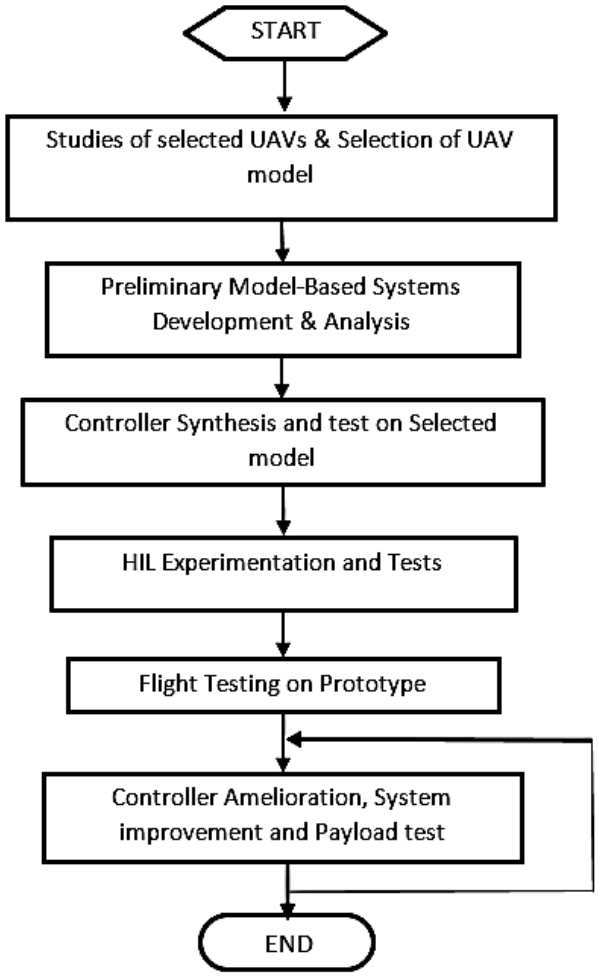

Figure 2: Proposed Development Workflow

4.2. UAV Types

The definition of Unmanned Aerial Vehicle Systems (UAVS) is made based on the structure of the airframe (fixed wing, rotary wing or hybrid), type of propulsion (hydrocarbon or air), take-off procedure (VTOL, HTOL) etc. These various types have their merits and demerits which include speed, maneuverability, ease of design, stability etc. Table I summarizes some characteristics of these two UAV types

Table I: UAV Comparison

	Design	***speed***	***maneuverability***	***control***
Fixed wing	***complex***	***high***	***intermediate***	***Intermediate to complex***
Rotary wing	***simple***	***modest***	***complex***	***simple***

Key: simple(s), intermediate (i) & complex(c), high, modest, slow

Fixed wing UAVs were previously the more commonly studied and utilized UAV type by actors such as the military. However, recent advances in robotics and algorithm development, is

creating renewed interest in rotary wing UAVs with a major shift towards multi-rotor type systems such as tri-, quad-,hexa- and octa-rotors. These multi-rotor systems being studied because they permit wide ranging types of control algorithms, possess extra design and operational redundancy. They are also uniquely suited for studies of multiple sensors, actuators and intelligence integration, therefore posing a challenging control question [17].

5. QUAV Model

The quadrotor unmanned aerial vehicle (QUAV) was adopted for this work because of its ability to teach core robotic systems concepts, permit quick development times, multiplicity of control algorithms and ease of understanding the system. It is modelled after Lagrangian principles [17] [22] with the dynamic model consisting of equations that allow for 6 DOF motion of the QUAV [15] [21].

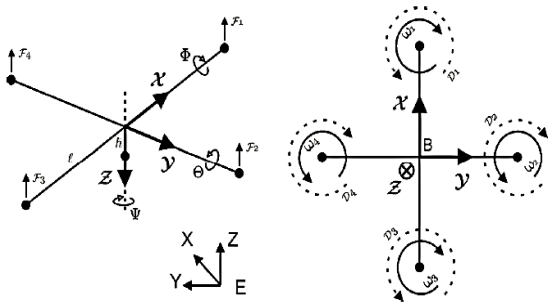

Figure 3: QUAV Dynamic Diagram [17]

These 6DOF represents the three translations and three rotations, along and about the x-, y- and z-axes respectively. Considering the forces, torques, rotations and velocities in Figure 3 as vectors, their respective directions are shown with respect to the working reference frames.

The structure of the QUAV requires opposite rotors to rotate in the same direction and in counter-rotation to the other two sets of rotors. This means when rotors 1 and 3 are rotating clockwise, rotors 2 and 4 will be rotating counter-clockwise. This rotation sequence gives stability and control properties to the vehicle structure during flight that would otherwise have required more complex algorithms to achieve compared to a fixed wing vehicle. Differential application of velocity on the rotors bringing about needed torques to control the QUAV for the principal maneuvers of roll(x axis rotation), pitch(y axis rotation) and yaw (z axis rotation).

A representative model was adopted from [17] which shows the dynamics of the attitude and translational component of the QUAV given by a nonlinear model.

$$
\begin{aligned}
I_{xx}\ddot{\phi} &= \dot{\theta}\dot{\psi}(I_{yy}-I_{zz}) + J_r\dot{\theta}\Omega_r + l(-T_2+T_4) - h(\sum_{i=1}^{4} H_{yi}) + (-1)^{i+1}\sum_{i=1}^{4} R_{mxi} \\
I_{yy}\ddot{\theta} &= \dot{\phi}\dot{\psi}(I_{zz}-I_{xx}) + J_r\dot{\phi}\Omega_r + l(T_1-T_3) - h(\sum_{i=1}^{4} H_{xi}) + (-1)^{i+1}\sum_{i=1}^{4} R_{myi} \\
I_{zz}\ddot{\psi} &= \dot{\theta}\dot{\phi}(I_{xx}-I_{yy}) + J_r\dot{\Omega}_r + (-1)^{i}\sum_{i=1}^{4} Q_i + l(H_{x2}-H_{x4}) + l(-H_{y1}+H_{y3}) \\
m\ddot{z} &= mg - (c\psi c\phi)\sum_{i=1}^{4} Ti \\
m\ddot{x} &= (s\psi s\phi + c\psi s\theta c\phi)\sum_{i=1}^{4} T_i - \sum_{i=1}^{4} H_{xi} - \frac{1}{2} C_x A_c \rho \dot{x}\,|\dot{x}| \\
m\ddot{y} &= (-c\psi s\phi + s\psi s\theta c\phi)\sum_{i=1}^{4} T_i - \sum_{i=1}^{4} H_{yi} - \frac{1}{2} C_y A_c \rho \dot{y}\,|\dot{y}|
\end{aligned}
\tag{1}
$$

Equation (1) represents the QUAV as six second order differential equations. However, adopting a state space approach, all possible situations which could arise in the UAV are descried

with respect to spatial position, angular displacements and velocities. This was captured by the state space vector defined as; $x = (\phi, \dot{\phi}, \theta, \dot{\theta}, \psi, \dot{\psi}, z, \dot{z}, x, \dot{x}, y, \dot{y})$, where x ϵ X, the set of all possible states [20-18]. Introducing new state variables for a more homogenous UAV dynamics model, the reordered dynamic system uses the state variables, x=x_1, x_2, x_3, x_4, x_5, x_6, x_7, x_8, x_9, x_{10}, x_{11}, x_{12}. The new variables were used to represent the QUAV as twelve first order dynamic equations.

$$
\begin{aligned}
\dot{x}_1 &= x_2 \\
\dot{x}_2 &= x_4 x_6 (I_{yy} - I_{zz}) / \mathrm{I}_{xx} + J_r / I_{xx} x_4 \Omega_r + l / I_{xx} U_2 \\
\dot{x}_3 &= x_4 \\
\dot{x}_4 &= x_2 x_6 (I_{zz} - I_{xx}) / I_{yy} + J_r / I_{yy} x_2 \Omega_r + l / I_{yy} U_3 \\
\dot{x}_5 &= x_6 \\
\dot{x}_6 &= x_4 x_2 (I_{xx} - I_{yy}) / I_{zz} + J_r / I_{zz} \dot{\Omega}_r + (-1)^{\mathrm{i}} / I_{zz} U_4 \\
\dot{x}_7 &= x_8 \\
\dot{x}_8 &= g - (c\psi c\phi) / \mathrm{mU}_1 \\
\dot{x}_9 &= x_{10} \\
\dot{x}_{10} &= (s\psi s\phi + c\psi s\theta c\phi) / \mathrm{mU}_1 \\
\dot{x}_{11} &= x_{12} \\
\dot{x}_{12} &= (-c\psi s\phi + s\psi s\theta c\phi) / \mathrm{mU}_1
\end{aligned}
\tag{2}
$$

The simplified system in (2) was utilized in controller synthesis which is presented next.

6. Controller design

Three controller types were tested with the QUAV model. The PID controller served as a baseline controller and was obtained from Matlabs continuous systems toolbox set and automatically tuned. A second controller was the Lyapunov based controller, while the third and final controller is the adaptive backstepping controller.

6.1. PID Control

Standard PID models are well known with little variation in the controller structure.

$$
\mathrm{U}_{\mathrm{pid}} = (K_p + K_i \frac{1}{s} + K_d \frac{d}{dt}) e(t) \tag{3}
$$

In Table II, Proportional (Kp), Integral (Ki) and Derivative (Kd) constants or gains for the roll, pitch, yaw and altitude controllers were obtained for the PID controller parameters:

Table II: PID Controller Gains

PID Gains	Roll	Pitch	Yaw	Z
Kp	-0.006055	-0.006055	-0.002591	0.120692
Ki	-0.000283	-0.000283	-0.00004537	0.005650
Kd	-0.031758	-0.031758	-0.012762	0.633049
Filter coefficient	5.454	5.454	114.283	5.454

The following gains were applied and for control law development that had (2) as target system.

6.2. Lyapunov Controller Design

Following the classic work of A.M. Lyapunov [1], Lyapunov stability theory has served as a cornerstone of most control stability work and control law development tasks for nonlinear systems. Applying this theory for the QUAV stability and convergence studies [16], the system states, x_1, x_3, x_5 were first identified for stabilization and control. Expressing them in the form of the well-known Lyapunov quadratic function structure [1] [16].

$$V(X_e)=\frac{1}{2}\left((x_1-x_{1d})^2+x_2^2+(x_3-x_{3d})^2+x_4^2+(x_5-x_{5d})^2+x_6^2\right) \tag{4}$$

Equation (4) contains the error terms and necessary states for stabilization. Taking the first derivative of equation (4), the following negative definite equation is obtained

$$\begin{aligned}\dot{V}(\mathrm{X}_e)&=(\mathrm{x}_1-\mathrm{x}_{1\mathrm{d}})\,\mathrm{x}_2+\mathrm{x}_2\frac{l}{I_{xx}}U_2+\\&(\mathrm{x}_3-\mathrm{x}_{3\mathrm{d}})\,\mathrm{x}_2+\mathrm{x}_4\frac{l}{I_{yy}}U_3+\\&(\mathrm{x}_5-\mathrm{x}_{5\mathrm{d}})\,\mathrm{x}_6+\mathrm{x}_6\frac{l}{I_{zz}}U_4\end{aligned} \tag{5}$$

With equation (5) being strictly negative definite (SND) ($\dot{V}<0$), it is seen that stabilizing state variable pairs (x_1, x_2), (x_3, x_4) and (x_5, x_6), demands that each subsystem have an extra SND term added. This extra terms are given by $-k_1x_2^2$, $-k_2x_4^2$, $-k_3x_6^2$. The obtained control laws after simplification of (5) becomes:

$$\begin{aligned}U_2&=-\frac{I_{xx}}{l}(x_1-x_{1d})-k_1x_2\\U_3&=-\frac{I_{yy}}{l}(x_3-x_{3d})-k_2x_4\\U_4&=-I_{zz}(x_5-x_{5d})-k_3x_6\end{aligned} \tag{6}$$

Similarly control laws were synthesized for the translational components z, x and y represented in the QUAV state space by x_7, x_8…x_{12}. The following controls were obtained and used in simulation

$$\begin{aligned}u_{1z}&=-\left(\frac{m}{mg-trigz}\right)(\mathrm{x}_7-\mathrm{x}_{7\mathrm{d}})-\mathrm{k}_4\mathrm{x}_8\\u_{1x}&=-\frac{m}{trigx}(\mathrm{x}_9-\mathrm{x}_{9\mathrm{d}})-\mathrm{k}_5\mathrm{x}_{10}\\u_{1y}&=-\frac{m}{trigy}(\mathrm{x}_{11}-\mathrm{x}_{11\mathrm{d}})-\mathrm{k}_6\mathrm{x}_{12}\end{aligned} \tag{7}$$

The parameters trigz=cψcϕ, trigx=sψsϕ+cψsθcϕ and trigy=-cψsϕ+sψsθcϕ respectively. They represent the trigonometric terms used in (1).

Where all the gains in (6) and (7) given by ki, i=1, 2… 6 are all positive definite constants. It is trivial to check that the final control laws are stabilizing, therefore this is left out here.

6.3. Backstepping Control law Design

The backstepping controller was another modern adaptive nonlinear control law used for the control parameter identification for the UAV. Extensive utilization of this technique is well documented in [17] [22] [19] for autonomous vehicles. Omitting the design details, the backstepping control for the QUAV has the following control laws synthesized:

$$U_2 = \frac{I_{xx}}{l}(-\alpha_2 e_2 - x_4 x_6 I_{yzx} - \frac{J_r}{I_{xx}} x_4 \Omega_r + \ddot{x}_1 - \frac{\dot{e}_1}{e_2}(e_1 - \alpha_1 e_2))$$
$$U_3 = \frac{I_{yy}}{l}(-\alpha_4 e_4 - x_4 x_2 I_{zxy} - \frac{J_r}{I_{xx}} x_2 \Omega_r + \ddot{x}_3 - \frac{\dot{e}_3}{e_4}(e_3 - \alpha_3 e_4)) \quad (8)$$
$$U_4 = I_{zz}(-\alpha_6 e_6 - x_4 x_2 I_{xyz} - \frac{J_r}{I_{zz}} \dot{\Omega}_r + \ddot{x}_5 - \frac{\dot{e}_5}{e_6}(e_5 - \alpha_5 e_6))$$

Implementation of the backstepping controller required some standard assumptions be made. The constants given by α_i are strictly positive, while the fractional error terms are approximated by constants that can also be selected arbitrarily at first and later tuned for optimality. Although not utilized at this stage of the work, optimization techniques such as mentioned in section (I-B) can be applied in obtaining optimum gain values for the constants α_i.

Similarly, controller synthesis was made for the translational dynamic of the system with the following derived results:

$$U_{1z} = -\left(\frac{M}{cx_5 cx_1}\right)(-\alpha_8 e_8 - \frac{\dot{e}_7}{e_8}(e_7 - \alpha_7 e_8) + \ddot{x}_{7d} - g)$$
$$U_{1x} = \left(\frac{M}{trigx}\right)(-\alpha_{10} e_{10} - \frac{\dot{e}_9}{e_{10}}(e_9 - \alpha_9 e_{10}) + \ddot{x}_{9d}) \quad (9)$$
$$U_{1y} = \left(\frac{M}{trigy}\right)(-\alpha_{12} e_{12} - \frac{\dot{e}_{11}}{e_{12}}(e_{11} - \alpha_{11} e_{12}) + \ddot{x}_{11d})$$

7. Simulation, Results and analysis

The QUAV system for simulation had the parameters defined in Table III.

Table III: QUAV Parameters

Parameter	Value	Unit	Description
Propeller parameters			
mp=	5.2	Kg	Kg
b=	3.13e-5		Thrust coefficient
d=	7.5e-7		Drag coefficient
Jr=	6e-5	Kg-m2	Rotor inertia
Motor parameters			
eta_mot	64		Motor efficiency
m_mot	12	Kg	Motor mass
R_mot	0.6	Ohm	Internal resistance
Jm	4e-7	Kg-m2	Motor inertia
Kem	5.2	Volt/rad/sec	EMF constant
Ki		Nm/A	
max_vel	600	rpm	Maximum rpm
QUAV Parameters			
M	0.650	Kg	QUAV mass
Ixx	7.5e-3	Kg-m2	Principal Body inertia
Iyy	7.5e-3	Kg-m2	"
Izz	1.3e-2	Kg-m2	"
Rrad	0.15	m	Blade radius
C	0.04	m	Chord length
L	0.23	m	Arm length

The following results are obtained from simulation experiments when each of the three controllers were used. The main system parameters which are shown are the roll, pitch and yaw response, and also the control torques generated by each controller for the various maneuver types.

7.1. PID Plot Group

Figure 4, 5 and 6 give the results for PID control of the three attitude angles ϕ, θ and ψ. These angles representing roll, pitch and yaw define the principal angular positions or orientations of the QUAV body with respect to a fixed frame of reference.

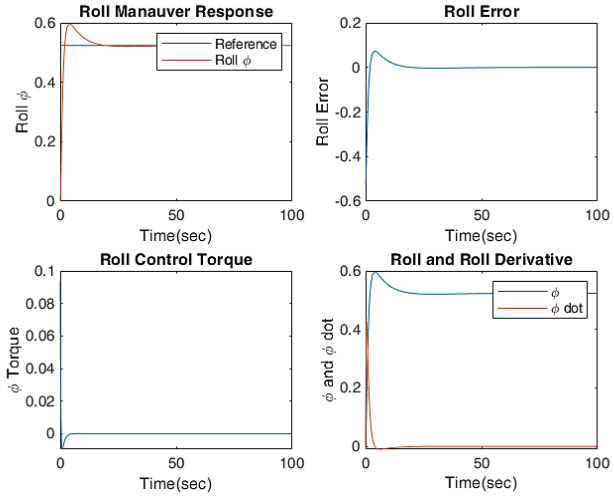

Figure 4: Roll Attitude Response from PID Controller

The system response to the PID controller is shown for the roll angular reference of pi/6 or 0.524 radians. Profiles of the error, torque and roll angle derivative are also given in Figure 4.

Figure 5 depicts the same set of response parameters for a pitch angular command of pi/4 or 0.785 radians.

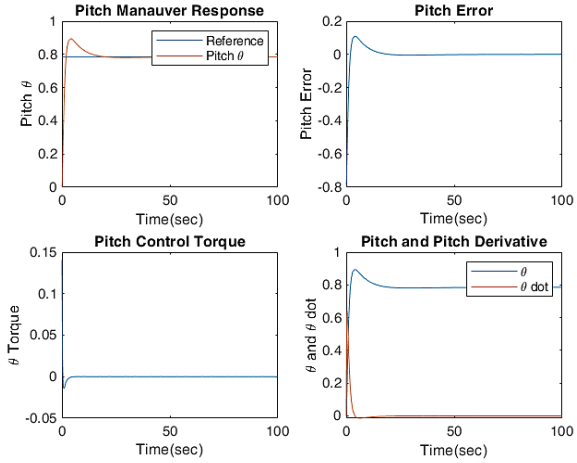

Figure 5: Pitch Attitude Response from PID Controller

Figure 6 gives the plot group for yaw command of pi/8 or 0.393 radians.

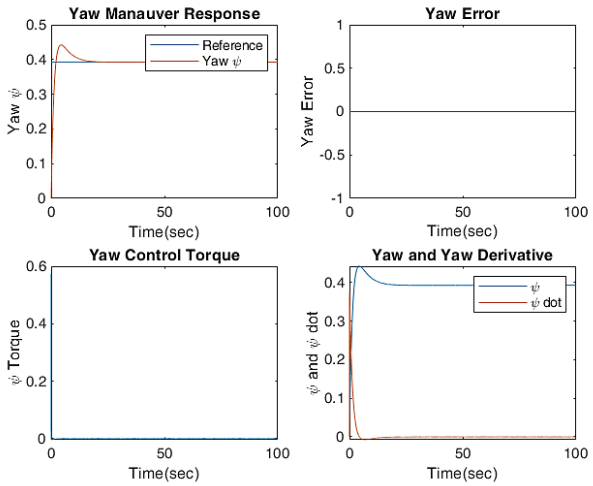

Figure 6: Yaw Attitude Response from PID Controller

Matlabs' stepinfo command was executed for each of the output responses. Table IV summarizes the results from the PID controller.

Table IV: PID Response Characteristics

Characteristic	Roll	Pitch	Yaw
RiseTime	70.091	70.313	83.070
SettlingTime	766.689	767.122	721.725
SettlingMin	0.473	0.707	0.355
SettlingMax	0.597	0.895	0.442
Overshoot	13.995	13.995	12.578
Undershoot	0.000	0.000	0.000
Peak	0.597	0.895	0.442
PeakTime	228.0	230.0	251.000

Overshoot values recorded for the PID controller, especially in the transient phase show similar magnitudes. Table IV shows no undershoot, while peak values are 0.597, 0.895 and 0.442 for the roll, pitch and yaw respectively responses with the PID.

7.2. Lyapunov Controller Plot Group

Figure 7, 8 and 9 give the results for Lyapunov control of the three attitude angles ϕ, θ and ψ. With the Lyapunov controller, the tunable gains K_i, with i=1, 2… 6 were arbitrarily set as k1=0.5; k2=0.5; k3=0.3; k4=0.0015; k5=0.25; k6=0.4. The only condition required to be satisfied being that each k_i is strictly greater than zero (k_i> 0) or each k_i must be a positive constant. Subsequently, these gains can be fine-tuned either offline or in real-time using any of the already mentioned optimization techniques in Section I-B.

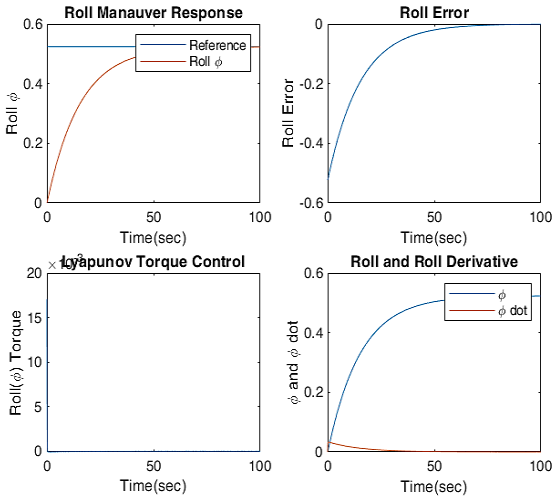

Figure 7: Roll Attitude Response from Lyapunov Controller

Figure 7 shows the response of the QUAV to roll command of pi/6 or 0.524 radians. Obvious from the plots is the complete non-existence of overshoot at the initial transient phase. Steady state error was completely absent which meant perfect tracking of the reference signal. These results are summarized in Table V.

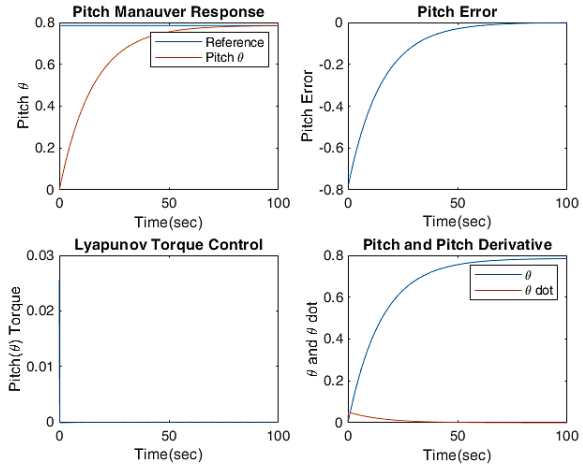

Figure 8: Pitch Attitude Response from Lyapunov Controller

Figure 8 gives similar sets of plots for the pitch response using the Lyapunov controller. For a pitch command of pi/4 or 0.7854 radians, the response featured zero overshoot, zero steady state error but large risetime.

Figure 9 was also having similar response profile with a Yaw command of pi/8 or 0.393 radians

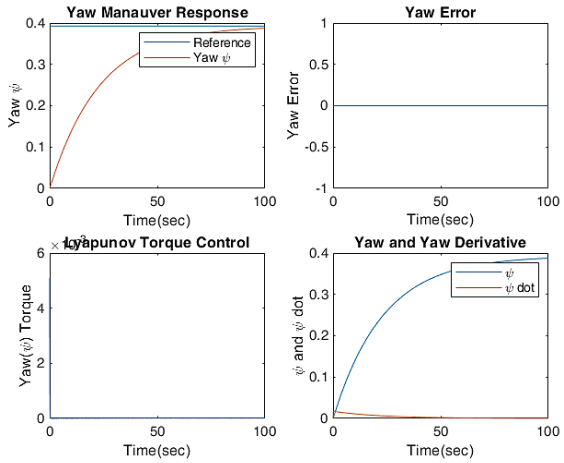

Figure 9: Yaw Attitude Response from Lyapunov Controller

Table V summarizes the results from the Lyapunov controller.

Table V: Lyapunov Controller Response Characteristics

Characteristic	Roll	Pitch	Yaw
RiseTime	153.575	153.569	333.824
SettlingTime	281.964	282.090	558.234
SettlingMin	0.471	0.707	0.349
SettlingMax	0.523	0.784	0.388
Overshoot	0.000	0.000	0.000
Undershoot	0.000	0.000	0.000
Peak	0.523	0.784	0.388
PeakTime	472.0	472.0	706.0

Zero overshoot and zero undershoot was recorded for the Lyapunov controller. No transient phase perturbations is present from Figure 7, 8 and 9. Table V, also recorded peak response values of 0.523, 0.784 and 0.388 respectively for the roll, pitch and yaw respectively maneuvers.

7.3. Backstepping Plot Group

Figure 10, 11 and 12 give the results for nonlinear backstepping control of the three attitude angles ϕ, θ and ψ which is also implemented and tested on the UAV model.

The backstepping model used the following parameters for manual fine-tuning of the control law; α_1=0.1, α_2=0.35, α_3=0.1, α_4=0.15, α_5=0.2, α_6=0.6, were selected as parameters for the attitudinal torque controllers while α_1=0.4, α_2=0.5, α_3=0.65, α_4=0.75, α_5=0.85, α_6=0.95, were selected as parameters for the translational control law constants.

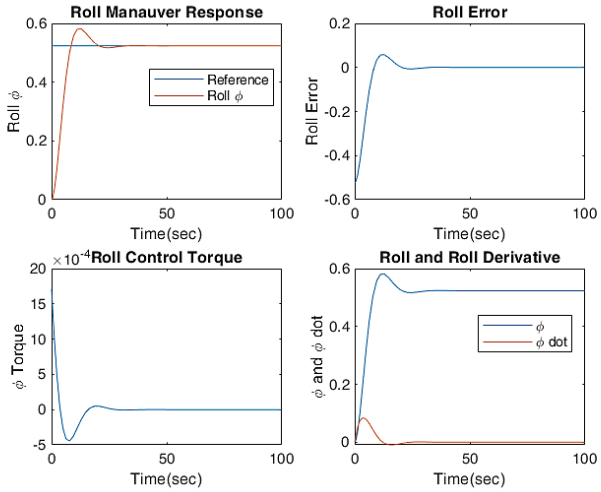

Figure 10: Roll Attitude Response from Backstepping Controller

The plots shown in Figure 10 were obtained for the backstepping controller roll command response.

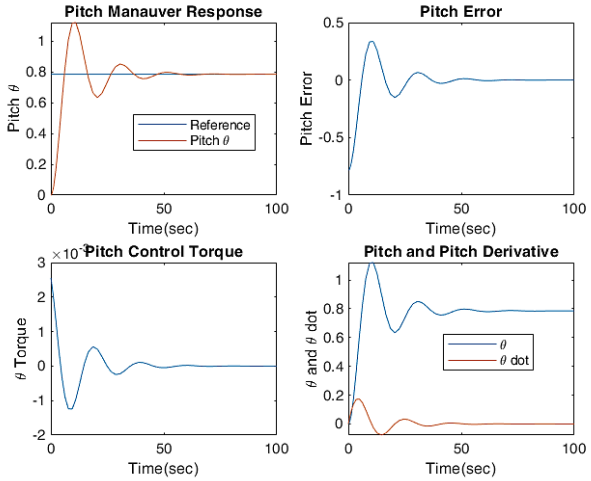

Figure 11: Pitch Attitude Response from Backstepping Controller

Figure 11 represents the pitch command response for the backstepping controller.

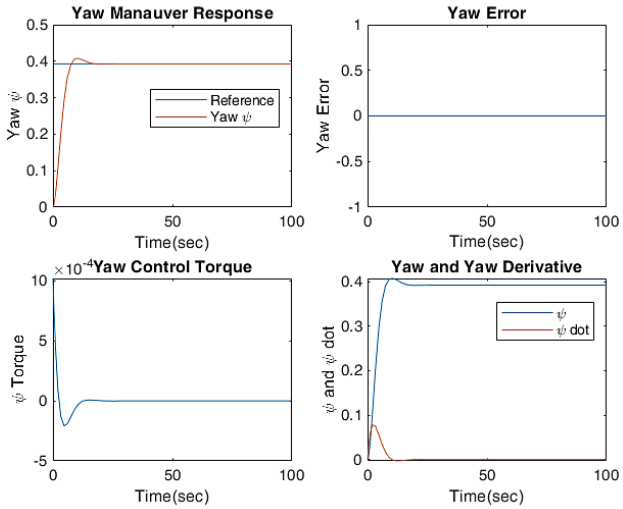

Figure 12: Yaw Attitude Response from Backstepping Controller

Finally the yaw response for the backstepping controller was also plotted as shown in Figure 12.

Table V summarizes the results from the backstepping controller.

Table VI: Backstepping Response Characteristics

Characteristic	**Roll**	**Pitch**	**Yaw**
RiseTime	4.6985	3.4389	4.2727
SettlingTime	22.2688	35.4819	19.2895
SettlingMin	0.475	0.637	0.379
SettlingMax	0.582	1.130	0.408
Overshoot	11.166	43.921	3.986
Undershoot	0.000	0.000	0.000
Peak	0.582	1.130	0.408
PeakTime	18.0	17.0	17.0

Significant overshoot was recorded for the backstepping controller, especially in the transient phase. Table V shows the pitch response had the highest overshoot value followed by the roll and yaw respectively.

8. System TORQUE Identification

In order to identify the control signal magnitudes for input into the QUAV dynamic system, the values for the control torques are characterized in both the transient and steady phase. This is to give better insight for further system development when incorporating the physical hardware described in the Figure 1.

Control torques as computed from the various responses when PID controller was used is recorded in Table VII

Table VII: Torque Characterization for PID Controllers

PID Control	Maximum values	Minimum values	**Steady state value**
Roll torque	93.8622e-003	-9.5647e-003	0
Pitch torque	140.7933e-003	-14.3678e-003	0
Yaw torque	573.7720e-003	-3.6965e-003	0
Total thrust	11.1622e+000	-554.1608e+000	

Control torques computed from the various responses when the Lyapunov controller was used is recorded in Table VIII

Table VIII: Torque Characterization for Lyapunov Controller

Lyapunov Control	**Maximum values**	**Minimum values**	**Steady state value**
Roll torque	17.0739e-003	-68.6582e-006	0
Pitch torque	25.6108e-003	-102.8822e-006	0
Yaw torque	5.1051e-003	-9.0188e-006	0

Finally, control torques as computed from the backstepping controller is recorded in Table IX. The recorded values are for the maximum and minimum control torques generated;

TABLE IX: Torque Characterization for Backstepping Controllers

Backstepping Control	Maximum values	Minimum values	Steady state value
Roll torque	1.7074e-003	-445.2817e-006	0
Pitch torque	2.5611e-003	-1.2452e-003	0
Yaw torque	1.0210e-003	-207.6699e-006	0

The magnitude of torque generated per maneuver is summarized in table

Table X: Summary of Control torque Effort par Maneuver

	Roll torque	Pitch torque	Yaw torque
PID control	93.8622e-003	140.7933e-003	573.7720e-003
Lyapunov control	17.0739e-003	25.6108e-003	5.1051e-003
Backstepping control	1.7074e-003	2.5611e-003	1.0210e-003

The torque values were represented as a pie chart to gain insight into the relative scale of control effort and energy needed per maneuver for each controller. This is shown in Figures 13

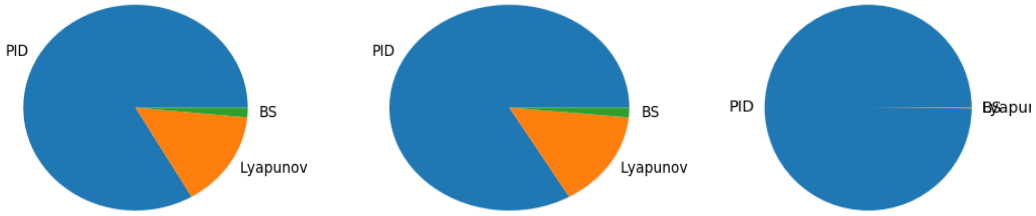

Figure 13: Relative Control Torque at Transient Regime

From the summary of torque generated per controller as given in Tables VII, VIII and IX, the nonlinear backstepping controller gives the best transient torque profile with results presented in Table IX. The backstepping controller presented the least maximum torque of all responses compared to the PID and Lyapunov controllers. This was followed by the Lyapunov controller and finally the PID controller. This conclusion was made with respect to aggregate control effort needed to achieve same command tracking maneuvers. This result gives added confidence and validates the choice for purely nonlinear controllers' adoption in this work. Subsequent work will entail utilization of purely nonlinear controllers with added optimization by parameter tuning. Furthermore, considering the energy constraints of current UAVs, utilizing such nonlinear controllers will add to battery savings, extend flight time per charge and payload sizing.

Conclusion

This work has identified three different controllers that are implemented for testing the control laws on a quadrotor UAV model. Using Matlabs stepinfo function, a first take at what constitutes good system response was made. The Lyapunov controller outperformed both the standard PID in terms of no overshoot and also the nonlinear backstepping controller in terms of overshoot but performs poorly when rise time and steady state response time is considered. However considering energy conservation with torque as the operative variable, the nonlinear backstepping controller outperformed both the PID and Lyapunov controllers. This has made nonlinear controller development the adopted control scheme for the long term goals of this project

as stated in section I-C. Furthermore, this work has opened up a research opportunity in control law development for the proposed QUAV experimental testbed.

This current research effort started in this paper will effectively be conducted at the Advanced Unmanned Aerial Vehicle research center of the NASRDA. Future work for advancement of the project will follow the workflow chart given in Figure 2. However, ongoing work not reported in this paper constitutes improvements to the control laws in order to accommodate robustness, adaptability and optimality. These improvements entail utilization of other control policies such as sliding mode control, output feedback and immersion invariance control schemes. Although not used in the preliminary tests described here, future work will also accommodate AI and CI nature inspired optimization schemes [2] to fine-tune selected UAV parameters for optimum performance. At each stage the controllers are discretized to gain insight into their digital implementation structure.

References

[1] A. M. LYAPUNOV, "The general problem of the stability of motion," INT. J. CONTROL, 1992, VOL. 55, No.3, 531-773

[2] A. T. Salawudeen, B. M. Mu'azu, Y. A. Sha'aban and C. J. Chan, "Optimal Design of PID Controller for Deep Space Antenna Positioning Using Weighted Cultural Artificial Fish Swarm Algorithm,". Journal of Electrical & Electronic Systems 2017, Vol 6(4)

[3] B. Zhao, B. Xian, Y. Zhang, and X. Zhang, "Nonlinear Robust Adaptive Tracking Control of a Quadrotor UAV via Immersion and Invariance Methodology," IEEE TRANSACTIONS ON INDUSTRIAL ELECTRONICS.

[4] C.C. Bissell, "A history of automatic control, "Springer Handbook of Automation, 2009

[5] C. Wu, "Robust Output Feedback Position Control for Quadrotor Based on Disturbance Observer," Proceedings of the 2015 IEEE Conference on Robotics and Biomimetics Zhuhai, China, December 6-9, 2015

[6] E. Hayden, M. Assante,T. Conway, "An abbreviated history of automation and industrial control systems and cybersecurity," A SANS Analyst Whitepaper. August 2014

[7] ISO 8373:2012 Robots and robotic devices - Vocabulary; http://www.iso.org/iso/iso_catalogue/catalogue_tc/catalogue_detail.htm?csnumber=55890.

[8] IFR, "The Impact of Robots on Productivity, Employment and Jobs," A positioning paper by the International Federation of Robotics April 2017

[9] M. D. Hua, T. Hamel, P. Morin, C. Samson, "Introduction to Feedback Control of Underactuated VTOL Vehicles," 2013 ACLI

[10] McKinsey Global Institute, "A Future That Works: Automation, Employment, And Productivity," McKinsey Global Institute. JANUARY 2017. EXECUTIVE SUMMARY

[11] N. S. Ozbek, M. Onkol and M. O. Efe, "Feedback control strategies for quadrotor-type aerial robots: a survey," Transactions of the Institute of Measurement and Control pp 1-26 DOI: 10.1177/0142331215608427

[12] O. Magnussen, M. Ottestad, G. Hovland, "Multicopter Design Optimization and Validation," Modeling, Identification and Control, Vol. 36, No. 2, 2015, pp. 67

[13] P. S. Sánchez and F. R. Cortés, "Cartesian Control for Robot Manipulators," Intech Open Journal

[14] R. Abbas and Q. Wu, "Improved Leader Follower Formation Control for Multiple Quadrotors Based AFSA," TELKOMNIKA, Vol.13, No.1, March 2015, pp. 85-92

[15] R. R. Serrezuela, A. F. C. Chavarro, M. A. Tovar Cardozo, A. L. Toquica and L. F. O. Martinez, "Kinematic Modelling Of A Robotic Arm Manipulator Using MATLAB," ARPN Journal of Engineering and Applied Sciences Vol. 12, NO. 7, APRIL 2017, pp 2037-2045

[16] R. I. Leine, "The historical development of classical stability concepts: Lagrange, Poisson and Lyapunov stability," Nonlinear Dynamics (2010) 59: 173–182

[17] S. Bouabdallah and R. Siegwart, "Full Control of a Quadrotor, "Autonomous Systems Lab. Swiss Federal Institute of Technology, ETHZ, Zurich, Switzerland

[18] S. M. LaValle, "Planning Algorithms," University of Illinois Copyright Steven M. LaValle 2006, pp 27-28

[19] T. I. Fossen and J. P. Strand, "Tutorials on Nonlinear Backstepping: Applications to ship control," Modelling identification and control. 1999, Vol 20(5), pp 83-134

[20] T. N. Dief and S. Yoshida, “System Identification for Quad-rotor Parameters Using Neural Network, ” EVERGREEN Joint Journal of Novel Carbon Resource Sciences & Green Asia Strategy, Volume 03, Issue 01, pp. 6-11, March 2016

[21] Y. R. Tang and Y. Li, “Dynamic Modeling for High-performance Controller Design of a UAV Quadrotor, ” Proceeding of the 2015 IEEE International Conference on Information and Automation Lijiang, China, August 2015

[22] Y. Sugawara and A. Shimada. “Attitude Control of Quadrotor in Consideration of the Effects of a Pole Based on Limited Pole Placement,” Electrical Engineering in Japan, Vol. 198, No. 1, 2017. Translated from Denki Gakkai Ronbunshi, Vol. 135-D, No. 8, August 2015, pp. 827–835

[23] Zulu and S. John, “A Review of Control Algorithms for Autonomous Quadrotors,” Open Journal of Applied Sciences, Vol 4, pp 547-556

[24] Z. T. Dydek, A. M. Annaswamy, and E. Lavretsky, “Adaptive Control of Quadrotor UAVs: A Design Trade Study With Flight Evaluations,” IEEE Transactions on Control Systems Technology. 2012